

Spin effects in a confined 2DEG: Enhancement of the g -factor, spin-inversion states and their far-infrared absorption.

Vidar Gudmundsson¹ and Juan José Palacios²

¹*Science Institute, University of Iceland, Dunhaga 3, IS-107 Reykjavik, Iceland.*

²*Department of Physics, Swain Hall West 117, Indiana University at Bloomington, IN 47405, USA.*

(January 23, 2018)

Abstract

We investigate several spin-related phenomena in a confined two-dimensional electron gas (2DEG) using the Hartree-Fock approximation for the mutual Coulomb interaction of the electrons. The exchange term of the interaction causes a large splitting of the spin levels whenever the chemical potential lies within a Landau band (LB). This splitting can be reinterpreted as an enhancement of an effective g -factor, g^* . The increase of g^* when a LB is half filled can be accompanied by a spontaneous formation of a static spin-inversion state (SIS) whose details depend on the system size. The coupling of the states of higher LB's into the lowest band by the Coulomb interaction of the 2DEG is essential for the SIS to occur. The far-infrared absorption of the system, relatively insensitive to the spin splitting, develops clear signs of the SIS.

71.70.Gm, 73.20.Dx, 75.30.Fv, 78.20.Ls

I. INTRODUCTION

The effects of the exchange interaction on the appearance of macroscopic spin structures have been studied in semiconductor microstructures in reduced dimensions by several researchers both theoretically and in experiments. The enhancement of the effective g -factor, g^* , of a two-dimensional electron gas (2DEG) in the quantum Hall regime has been reviewed by Ando, Fowler, and Stern.¹ For the unbounded 2DEG Ando and Uemura² presented a model where the broadening of the Landau levels due to impurity scattering is treated in the self-consistent Born approximation (SCBA). The dielectric function is calculated with the inclusion of the lowest order exchange energy of the screened Coulomb interaction in the self-energy of the electrons. For a strong magnetic field the overlapping of Landau levels with different indices is neglected.

The enhancement of g^* can lead to a spin polarization of the 2DEG at certain values of the filling factor ν , and, in addition, the exchange interaction can lead to the spontaneous formation of spin-density³ or charge-density waves^{4,5}. The onset of a spin-density wave state in a parabolic quantum well has been studied by Brey and Halperin using a modified Hartree-Fock approximation (HFA) with a point-contact exchange interaction. They find a divergence of the electric susceptibility in the presence of a magnetic field of intermediate strength parallel to the quantum well and an infinitesimal fictitious magnetic field perpendicular to the quantum well.⁶ This spin-density wave state has a wavevector along the quantum well parallel to the intermediate magnetic field and occurs only when the quantum well is wide enough and the exchange interaction has a strength larger than a critical value. The calculated optical properties of a δ -doped quantum well in the HFA due to spin- and charge-density excitations have been found to be in good agree-

ment with experiments,⁷ as well as those of donor states in 2DEG in strong magnetic fields.⁸ In the quantum well Hembree *et al.*⁹ discovered abrupt spin polarization of the system at high magnetic fields and a spin-inversion regime where the net spin alignment strongly varies across the well. They studied the effect in different approximation schemes and in the presence of impurity scattering. Recently the effects of the g -factor enhancement on various transport coefficients has been reported by the same group.¹⁰

As to microstructures of further reduced dimensionality the spontaneous polarization of of an array of quantum dots into a ferroelectric or antiferroelectric state has been investigated by Kempa, Broido, and Bakshi.¹¹ The spin degree of freedom together with the exchange interaction and correlation effects have also been found to be essential to model few electrons in a single quantum dot in magnetic field.^{12–16}

In this paper we are concerned with the spin-related phenomena associated with the exchange interaction that can occur in quantum dots with a large number of electrons. We study the spin splitting of Landau bands (LB's) due to the enhancement of g^* , and the formation of a spin-inversion state (SIS) in a strictly two-dimensional *finite size* electron system in a perpendicular magnetic field of intermediate strength. The system size is chosen to be of the order of several magnetic lengths, $l = \sqrt{\hbar c/(eB)}$. The LB's in the center of the system do approach flat Landau levels indicating that an electron in the center does not feel the boundary. We are thus able to study the crossing from the quantum regime in which the electronic confinement dominates over the electron-electron interaction to the regime in which electrostatics plays a dominant role. Finally we show how the formation of a SIS can be detected in the far-infrared (FIR) absorption spectrum of the system.

II. MODEL

We consider N_s strictly two-dimensional electrons to model qualitatively a real heterostructure where the 2DEG is confined to the lowest electrical subband. The 2DEG is confined to a disk of radius R in the 2D-plane by a potential step

$$V_{\text{conf}}(r) = U_0 \left[\exp\left(\frac{R-r}{4\Delta r}\right) + 1 \right]^{-1}, \quad (1)$$

where $\Delta r = 22 \text{ \AA}$. To ensure charge neutrality of the system a positive background charge $+en_b$ resides on the disk

$$n_b(r) = \bar{n}_s \left[\exp\left(\frac{r-R}{\Delta r}\right) + 1 \right]^{-1}, \quad (2)$$

with the average electron density of the system given by $\bar{n}_s = N_s/(\pi R^2) = \langle n_s(r) \rangle$. In the HFA the state of each electron is described by a single-electron Schrödinger equation

$$\begin{aligned} & \{H^0 + V_H(r) + V_{\text{conf}}(r)\}\psi_\alpha(\vec{r}) \\ & - \int d^2r' \Delta(\vec{r}, \vec{r}')\psi_\alpha(\vec{r}') = \epsilon_\alpha\psi_\alpha(\vec{r}) \end{aligned} \quad (3)$$

for an electron moving in a Hartree potential

$$V_H(r) = \frac{e^2}{\kappa} \int d^2r' \frac{n_s(r') - n_b(r')}{|\vec{r} - \vec{r}'|} \quad (4)$$

caused by the charge density $-e\{n_s(r) - n_b(r)\}$, and a nonlocal exchange potential with

$$\Delta(\vec{r}, \vec{r}') = \frac{e^2}{\kappa} \sum_{\beta} f(\epsilon_\beta - \mu) \frac{\psi_\beta^*(\vec{r}')\psi_\beta(\vec{r})}{|\vec{r} - \vec{r}'|}. \quad (5)$$

The equilibrium occupation of the electronic states is according to the Fermi distribution $f(\epsilon_\beta - \mu)$ at finite temperature T . The density of the electrons $n_s(r)$ is constructed from the energy spectrum $\{\epsilon_\alpha\}$ and the wave functions $\{\psi_\alpha\}$

$$n_s(r) = \sum_{\alpha} |\psi_{\alpha}(\vec{r})|^2 f(\epsilon_{\alpha} - \mu), \quad (6)$$

together with the chemical potential μ . The label α represents the radial quantum number n_r , the angular quantum number M , and the spin quantum number $s = \pm\frac{1}{2}$. H^0 is the single particle Hamiltonian for one electron with spin in a constant perpendicular external magnetic field.^{17,18} A Landau band index n can be constructed from the quantum numbers n_r and M as $n = (|M| - M)/2 + n_r$. The Landau levels of H^0 with energy $E_{n,M,s} = \hbar\omega_c(n + \frac{1}{2}) + sg^*(\mu_B/\hbar)B$ are degenerate with respect to M with the degeneracy $n_0 = (2\pi l^2)^{-1}$ per spin orientation. μ_B is the Bohr magneton ($e\hbar/2mc$). The cyclotron frequency is given by $\omega_c = eB/(mc)$. The Hartree-Fock energy spectrum $\{\epsilon_{\alpha}\}$ and the corresponding wave functions $\{\psi_{\alpha}\}$ are now found by solving (3)-(6) iteratively in the basis of H^0 .^{18,19,12} The chemical potential μ is recalculated in each iteration in order to preserve the total number of electrons N_s . The number of basis functions used in the diagonalization is chosen such that a further increase of the subset results in an unchanged density $n_s(r)$. The calculations have been repeated for several initial conditions with different spin configuration in order to search for the ground state of the Hartree-Fock equations (3)-(6). The total energy of the system E_{tot} can be found by summing up the single electron contributions and carefully counting the interaction energy of each electron pair only once.¹²

The FIR-absorption of the system is calculated as a self-consistent linear response to an external potential²⁰

$$\phi^{\text{ext}}(\vec{r}, t) = \mathcal{E}^{\text{ext}} r \exp\{-iN_p\varphi - i(\omega + i\eta)t\}, \quad (7)$$

where $\eta \rightarrow 0^+$. $N_p = \pm 1$ corresponds to left or right circular polarization. The small size of the system compared to the wavelength of the external radiation makes possible to use a electrostatic potential representing a time dependent but spatially constant external electrical field $\vec{E}^{\text{ext}} = -\vec{\nabla}\phi^{\text{ext}}$.

In this so-called time-dependent HFA the change of the density matrix due to an adiabatically switched-on total electrostatic potential ϕ^{SC} is calculated within a linear approximation. The total potential consists of the external potential and the induced potential $\phi^{\text{ind}} = \phi^H + \phi^F$ due to the direct and the exchange interaction of the electrons. The induced potential in turn depends on the density matrix, thus closing the circle and allowing for a self-consistent evaluation of the total potential together with an expression for the frequency dependent dielectric tensor $\varepsilon_{\alpha\beta,\delta\gamma}(\omega)$. The power absorption is then calculated from the Joule heating of the system due to ϕ^{ext}

$$P(\omega) = e\mathcal{E}^{\text{ext}} \sum_{\alpha\beta} \frac{(E_\beta - E_\alpha)}{\hbar} \langle \beta | r | \alpha \rangle 2\pi \delta_{M_\beta, M_\alpha \pm N_p} \Im \left\{ f^{\alpha\beta}(\omega) \langle \alpha | (-e\phi^{\text{SC}}) | \beta \rangle \right\}, \quad (8)$$

where \mathcal{E}^{ext} is the strength of the external field and

$$f^{\alpha\beta}(\omega) = \frac{1}{\hbar} \left\{ \frac{f_\beta - f_\alpha}{\omega + (\omega_\beta - \omega_\alpha) + i\eta} \right\} \quad (9)$$

with the Fermi distribution $f_\alpha = f(\epsilon_\alpha - \mu)$.

III. RESULTS

The calculations for the box-like confinement (1) are carried out with GaAs parameters: $m^* = 0.067m_e$, $\kappa = 12.4$, and $g^* = -0.44$. The occupation of the LB's is varied by changing the number of electrons N_s at a constant strength of the magnetic field $B = 3.0$ T (we could equally have changed the magnetic field keeping constant the number of particles). Since the radius of the system $R \geq 1000$ Å is much larger than the magnetic length $l \approx 148$ Å and the effective Bohr radius $a_0^* \approx 97.9$ Å we can use as a convenient label an effective filling factor ν describing the occupation of the LB's in the interior of the system. The cyclotron energy $\hbar\omega_c \approx 5.2$ meV, so a sufficient height of the confining potential is $U_0 = 60$ meV in order to include several LB's in the calculation. For $B = 3.0$ T the bare spin splitting of the LB's

$E_{\text{Zeeman}} = (g^* \mu_B / \hbar) B \approx 0.076 \text{ meV}$ is much smaller than their separation $\hbar\omega_c$ and corresponds to the thermal energy $k_B T$ at $T \approx 0.9 \text{ K}$.

Figure 1 shows the HFA quasiparticle energy spectrum for four values of N_s such that the filling factor ν (defined as the number of occupied bands in the central region of the box) ranges from 4 to 2. Figure 1a corresponds to the case $\nu = 4$. Electrons in the first LB ($n = 0$) form a large paramagnetic compact droplet while electrons in the second LB ($n = 1$) form a smaller one. Figures 1b and 1c show clearly a large spin splitting of the LB's due to the enhancement of g^* when the 2nd LB is half filled ($\nu = 3$) and the electrons in it form a ferromagnetic compact droplet. Finally, Fig. 1d shows the case corresponding to the droplet at $\nu = 2$ when no electrons are left in the 2nd LB. In our case the 2nd LB behaves in all respects like an independent, smaller quantum dot, and its properties are identical to those studied previously.¹⁵ However, the first LB present a more complicated behavior: The energy spectra for six values of N_s such that the chemical potential μ lies in the neighborhood of the first LB is seen in Fig. 2. Now the filling factor lies within the range $1 \leq \nu \leq 2$. For $N_s = 42$ (Fig. 2a) both spin bands of the first LB in the bulk region are still filled (μ is still lying between the first and second LB's but closer to the former one). The small Zeeman energy makes the LB's look degenerate with respect to the spin degree of freedom. As the number of electrons is reduced to 38 (Fig. 2b) the spin bands split up near the edge and the number of spin-down electrons becomes smaller than that of spin-up electrons. In addition to this splitting (which was also present in the 2nd LB in Fig. 1) we can observe two instability points (one for each spin band) rising near the center of the system. By instability points we mean bumps in the spin bands approaching the chemical potential. Thus, one should expect some transition as the number of electrons keeps changing (or the magnetic field) and these bumps touch the chemical potential. Before

that can happen one can even see signatures of such transitions in the density plotted in Fig. 3. The finite temperature "reveals" a budding spin-inversion state due to the difference in distance to the chemical potential between the spin-up and spin-down bands for a given position (M). The onset of such a SIS takes place when the number of particles is reduced further and those bumps cross the chemical potential (Figs. 2c to 2e). Finally, the compact droplet at $\nu = 1$ is formed (Fig. 2f).

In order to understand better the formation of the SIS let us consider a simpler but equivalent situation. The number of LB's cannot be reduced considerably in the calculations with the box-like confinement (1) since we are using a basis constructed of the eigenfunctions of noninteracting electrons in an infinite system. However, by considering parabolically confined interacting electrons and using the one-electron basis set of such a system we are left only with band mixing due to the electron-electron interaction. We have thus calculated the energy spectra of a 2DEG in a parabolic quantum dot with confinement frequency $\hbar\omega_0$ for an increasing number of LB's (from one to three) at $T = 1.0\text{K}$. First, we analyze the case of one LB at zero temperature. Figure 4 shows the evolution with B of the band structure for $N_s = 30$. The spin splitting opens up from the edge to the center of the LB in the parabolic confinement as we go from $\nu = 2$ to $\nu = 1$. Surprisingly, one can see how both spin bands near the center of the system bend upward, and, eventually, one of them crosses the chemical potential. This cannot happen for a smaller number of electrons since in that case the $s = -\frac{1}{2}$ electrons leave their band before the unstable point (in the center) crosses the chemical potential. Such central instability requires a certain size of the electronic droplet and constitutes the initial stage of the SIS. If we include higher LB's the spectra becomes more complicated and the instability points of each spin band shift from each other due to the mixing with higher LB's. This result is presented in Fig. 5. The

total energy of the system E_{tot} is 1789.07 meV for one LB, 1728.3 meV for two LB's, and 1718.5 meV for three. Obviously the calculation with one LB does not represent well the ground state for the given values of $\hbar\omega_c$ and $\hbar\omega_0$, but helps us to get an insight on the spin instability. *No twisting of the spin bands is ever seen for the calculation with one LB.* This can be verified by checking the analytical expressions for the matrix elements of the exchange interactions. The additional degree of freedom introduced to the system by allowing coupling of states of higher LB's into the lowest LB for interacting electrons is essential in order to obtain the full richness of the spin band structure.

The formation of the SIS invokes clear signs in the FIR spectrum $P(\omega)$ of the 2DEG detailed in Fig. 6. The first two subfigures show the spectrum in the Hartree approximation (HA) and the HFA, respectively. In the HA the exchange interaction is neglected both in the ground state and the excited states. A common feature is the occurrence of two strong absorption lines, the lower one in energy corresponding to $N_p = +1$ and the higher one corresponding to $N_p = -1$. These two lines can either be identified as the ones corresponding to the center of mass motion predicted by the generalized Kohn theorem for quantum dots with parabolic confinement,^{21–25} or more appropriately here as the low energy excitation of an edge plasmon and the 2D bulk plasmon at energy slightly higher than the cyclotron resonance $E_c = \hbar\omega_c$.²⁰ Both approximation then show small absorption peaks above the bulk magnetoplasmon that have been identified as absorption due to single electron transitions.^{26,20} The spin splitting itself does not have large effects on the absorption due to the bulk magnetoplasmon but the finer details of the corresponding absorption peak in a parabolic quantum well have been studied by Hembree et. al.,¹⁰ here we shall concentrate on the effects of the SIS. By comparing the spectra for the two approximations at energy below the energy of the edge plasmon

we find small peaks for $N_p = -1$ that are enlarged in the last subfigure of Fig. 6. No such peaks are found in the HA. They are only present when the SIS occurs and the ones with the lowest energy are caused by single electron transitions in the lowest LB, intra-Landau-band transitions with $M \rightarrow M - 1$ that are only possible because of the twisting of the LB's. Corresponding absorption peaks of the opposite polarization $N_p = +1$ can also be found in the center subfigure at similar energy, but the peaks with $N_p = -1$ are much more characteristic of the SIS since otherwise peaks of that polarization are never found for low energy. As soon as the spin Landau bands of the lowest LB cross twice a second absorption peak appears with energy above the edge magnetoplasmon but below the bulk plasmon. The occurrence of this second row of peaks has to be correlated with the fact that the twisting of the lowest and the next LB, that did mirror one another for lower N_s , are now out of phase for the higher values of N_s corresponding to ν just below 2.

IV. DISCUSSION AND SUMMARY

In a system of a confined 2DEG we have been able to demonstrate both bulk effects and phenomena caused by the finite size of the system, in the absence of any impurity scattering of the electrons. The 2D system is large enough so that the LB's approach flat Landau levels for low values of the angular quantum number M . This can be interpreted as the formation of 2D bulk states inside the system. The ensuing singular density of states together with the exchange interaction causes the well known oscillations of the energy separation of the LB's with the same Landau level index n but opposite spin orientations as a function of the filling factor ν . Here we have seen that the enhancement of g^* occurs not only in the LB where μ is located but in all the LB's included in the model. Similar behavior has been established in optical

measurements of a 2DEG by Kukushkin.²⁷

We have observed the spontaneous formation of concentric circular regions of different spin phases when the spin splitting of the first LB's is opening up with a decreasing ν at a low temperature. The shape of this SIS depends on the size, shape of the system, and filling factor ν , such that the wavelength decreases as ν approaches an even integer. The coupling of the states of higher Landau bands into the lowest band by the Coulomb interaction of the 2DEG is *essential* for the fine structure of the SIS.

Even though we have been using a restricted HFA here (total angular momentum and spin are good quantum numbers) different results can be attained by choosing different initial spin configurations. In Fig. 7 we show three stable states with higher energy than the ground state seen in Fig. 2c. It is interesting to note that the state with no crossing of spin bands is not the ground state.

The exact shape of the SIS does strongly depend on the confining potential and, thus, also the size of the system. As was noted earlier the LB's do not twist when μ is crossing higher LB's and the spin splitting is opening up, but the uneven opening up produces strong modulation of the spin densities. To exclude the possibility that numerical deficiencies are causing the twisting of the Landau bands we have tested the stability of the spin-density structures by increasing the number of basis states included in the numerical calculation and tested different schemes in attaining the convergence of the self-consistent problem. No visible changes in the ground state properties were observed. On the other hand, the exact shape and formation of the SIS does depend on the size of the system emphasizing that we are observing a confined spin-density wave (SDW) here.^{20,28}

Two possible problems associated with the HFA come to mind. First, the HFA may lead to a ground state that is quite different from the physical

one due to the strong exchange force that may be reduced in better approximations where higher order correlation effects or impurity broadening to a high order are included.²⁹ It is thus, very reassuring that this type of spin inversion and formation of a SDW has been observed in models employing the local density approximation (LDA) where the SDW has been observed for different approximations of the correlation effects.⁹ The on-set of the SDW is also found to depend on the amount of collision broadening of the LB's, but neither the broadening nor the correlation effects prevent it.⁹ The spatial correlation of the 2DEG in two approaching finite-size layers for the common filling factor of unity is quite similar to the formation of the SIS here. The layer index can be treated as isospin for vanishing separation and the numerical diagonalization of the many-electron Hamiltonian in a large subspace of noninteracting many-electron states includes, in principle, all correlation effects in the model to a high degree of accuracy.³⁰

An important difference of the present SIS in the two-dimensional plane to the SDW parallel to \vec{B} investigated by Brey and Halperin⁶ is the fact that the wavelength of the present modulation varies strongly with ν . This is caused by the strong dependence of the effective interaction, or the screening, in the 2D plane on ν .^{18,31–33} The SDW found by Brey and Halperin has strong resemblance with the more “traditional one” known in 1D electronic systems.³ The notation SIS is, therefore, used here to emphasize this difference.

The region of filling factors when the electrons are not fully spin polarized yet ($1 \leq \nu \leq 2$) but the system has not entered the regime of the integer quantum Hall effect with the lowest LB filled ($\nu = 1$) has attracted much interest lately. It has been shown that in absence of Zeeman energy the lowest energy charged excitations at $\nu = 1$ are skyrmions, spin textures with a unit winding number in two dimensions.^{34,35} At large g the quasi-particles,

analogous to the single particles, have unit charge $\pm e$ and spin half, $s = \pm 1/2$, but as g is reduced to zero the excitation gap survives and the size of the quasi-particles diverges with the spin becoming macroscopic - skyrmions.³⁵ This effect has also been studied in double-layered electron systems when the distance between the layers, each having no spin degree of freedom, is reduced since these models can be mapped directly onto the spin system identifying the layer index as an isospin.^{30,36} It has also been found that these spin textures might eventually dominate the ground state properties at filling factors $1 \leq \nu \leq 2$.^{15,30,37} The SIS's found in the present work are *not* related to the skyrmions observed in such regime of filling factors, but the skyrmions and the SIS's may coexist, which emphasizes the very complex and interesting structure of the 2DEG in such a regime.

The spin-density modulation was found to cause clear signs in the FIR-absorption of the confined 2DEG. The signs may be weak since they partly reflect single-electron transitions rather than collective oscillations and they may be in the low frequency part of the spectrum most difficult to measure, but the final word about the appropriateness of the HFA or the LDA for the current model will come from experiments.

ACKNOWLEDGMENTS

The authors are indebted to R. R. Gerhardts, D. Pfannkuche, A. H. MacDonald, M. Ferconi, G. Vignale, and G. Pálsson for fruitful discussion. This research was supported in part by the Icelandic Natural Science Foundation, the University of Iceland Research Fund, NATO collaborative research Grant No. CRG 921204, NFS contract nsf-dmr9416906, and, for one of the authors (J.J.P.), by a NATO postdoctoral fellowship.

REFERENCES

- ¹ T. Ando, A. B. Fowler, and F. Stern, *Rev. Mod. Phys.* **54**, 437 (1982).
- ² T. Ando and Y. Uemura, *J. Phys. Soc. Japan* **37**, 1044 (1974).
- ³ G. Grüner, *Rev. Mod. Phys.* **66**, 1 (1994).
- ⁴ R. R. Gerhardts, *Phys. Rev. B* **24**, 1339 (1981).
- ⁵ D. Yoshioka and P. Lee, *Phys. Rev. B* **27**, 4986 (1983).
- ⁶ L. Brey and B. Halperin, *Phys. Rev. B* **40**, 11634 (1989).
- ⁷ M. S.-C. Luo, S. L. Chuang, S. Schmitt-Rink, and A. Pinczuk, *Phys. Rev. B* **48**, 11086 (1993).
- ⁸ P. Hawrylak, *Phys. Rev. Lett.* **72**, 2943 (1994).
- ⁹ C. E. Hembree *et al.*, *Phys. Rev. B* **48**, 9162 (1993).
- ¹⁰ C. E. Hembree, B. A. Mason, J. T. Kwiatkowski, and J. E. Furneaux, *Phys. Rev. B* **50**, 15197 (1994).
- ¹¹ K. Kempa, D. Broido, and P. Bakshi, *Phys. Rev. B* **43**, 9343 (1991).
- ¹² D. Pfannkuche, V. Gudmundsson, and P. Maksym, *Phys. Rev. B* **47**, 2244 (1993).
- ¹³ D. Pfannkuche, R. Gerhardts, P. Maksym, and V. Gudmundsson, *Physica B* **189**, 6 (1993).
- ¹⁴ P. Hawrylak, *Phys. Rev. Lett.* **71**, 3347 (1993).
- ¹⁵ J. J. Palacios *et al.*, *Phys. Rev. B* **50**, 5760 (1994).
- ¹⁶ M. Ferconi and G. Vignale, *Phys. Rev. B* **50**, 14722 (1994).
- ¹⁷ L. D. Landau and E. M. Lifshitz, *Quantum Mechanics* (Pergamon Press, London, 1958).
- ¹⁸ V. Gudmundsson, *Solid State Comm.* **74**, 63 (1990).
- ¹⁹ V. Gudmundsson, in *Proceedings of the NATO Advanced Research workshop on Semiconductor*

- Microstructures, May 1989, Venezia*, edited by A. F. G. Fasol and P. Lugli (Plenum Press, New York, 1989), p. 517.
- ²⁰ V. Gudmundsson and Á. S. Loftsdóttir, *Phys. Rev. B* **50**, 17433 (1994).
- ²¹ W. Kohn, *Phys. Rev.* **123**, 1242 (1961).
- ²² P. A. Maksym and T. Chakraborty, *Phys. Rev. Lett* **65**, 108 (1990).
- ²³ L. Brey, N. Johnson, and B. Halperin, *Phys. Rev. B* **40**, 10647 (1989).
- ²⁴ V. Gudmundsson and R. Gerhardtts, *Phys. Rev. B* **43**, 12098 (1991).
- ²⁵ D. Pfannkuche, V. Gudmundsson, P. Hawrylak, and R. Gerhardtts, *Solid-State Electronics* **37**, 1221 (1994).
- ²⁶ A. G. Mal'shukov, A. Brataas, and K. A. Chao, *Phys. Rev. B* **51**, 7669 (1995).
- ²⁷ I. V. Kukushkin, S. V. Meshkov, and V. B. Timofeev, *Sov. Phys. Usp.* **31**, 511 (1988).
- ²⁸ V. Gudmundsson and G. Pálsson, *Physica Scripta T* **54**, 92 (1994).
- ²⁹ T. Uenoyama and L. J. Sham, *Phys. Rev. B* **39**, 11044 (1989).
- ³⁰ J. J. Palacios and P. Hawrylak, *Phys. Rev. B* **51**, 1769 (1995).
- ³¹ U. Wulf, V. Gudmundsson, and R. Gerhardtts, *Phys. Rev. B* **38**, 4218 (1988).
- ³² J. Labbé, *Phys. Rev. B* **35**, 1373 (1988).
- ³³ P. L. McEuen *et al.*, *Phys. Rev. B* **45**, 11419 (1992).
- ³⁴ S. L. Sondhi, A. Karlhede, S. A. Kivelson, and E. H. Rezayi, *Phys. Rev. B* **47**, 16419 (1993).
- ³⁵ H. A. Fertig, L. Brey, R. Côté, and A. H. Macdonald, *Phys. Rev. B* **50**, 11018 (1994).
- ³⁶ K. Moon *et al.*, *Phys. Rev. B* **51**, 5138 (1995).
- ³⁷ T. Schmidt *et al.*, *Phys. Rev. B* **51**, 5570 (1995).

FIGURES

FIG. 1. The ground state HFA energy spectra and chemical potential μ (horizontal line) for (a) $N_s = 82$, (b) $N_s = 62$, (c) $N_s = 52$, and (d) $N_s = 48$ electrons in the system. $T = 10.0$ K, $R = 1000$ Å, $U_0 = 60$ meV, and $B = 3.0$ T. Crosses represent the $s = +\frac{1}{2}$ electrons and diamonds represent $s = -\frac{1}{2}$. GaAs bulk parameters: $m^* = 0.067m_0$, $\kappa = 12.4$, $g^* = -0.44$.

FIG. 2. The ground state energy spectra and chemical potential μ (horizontal line) for (a) $N_s = 42$, (b) $N_s = 38$, (c) $N_s = 34$, (d) $N_s = 30$, (e) $N_s = 26$, and (f) $N_s = 22$ electrons in the system. $T = 4.0$ K, $R = 1000$ Å, $U_0 = 60$ meV, and $B = 3.0$ T. Crosses represent the $s = +\frac{1}{2}$ electrons and diamonds represent $s = -\frac{1}{2}$.

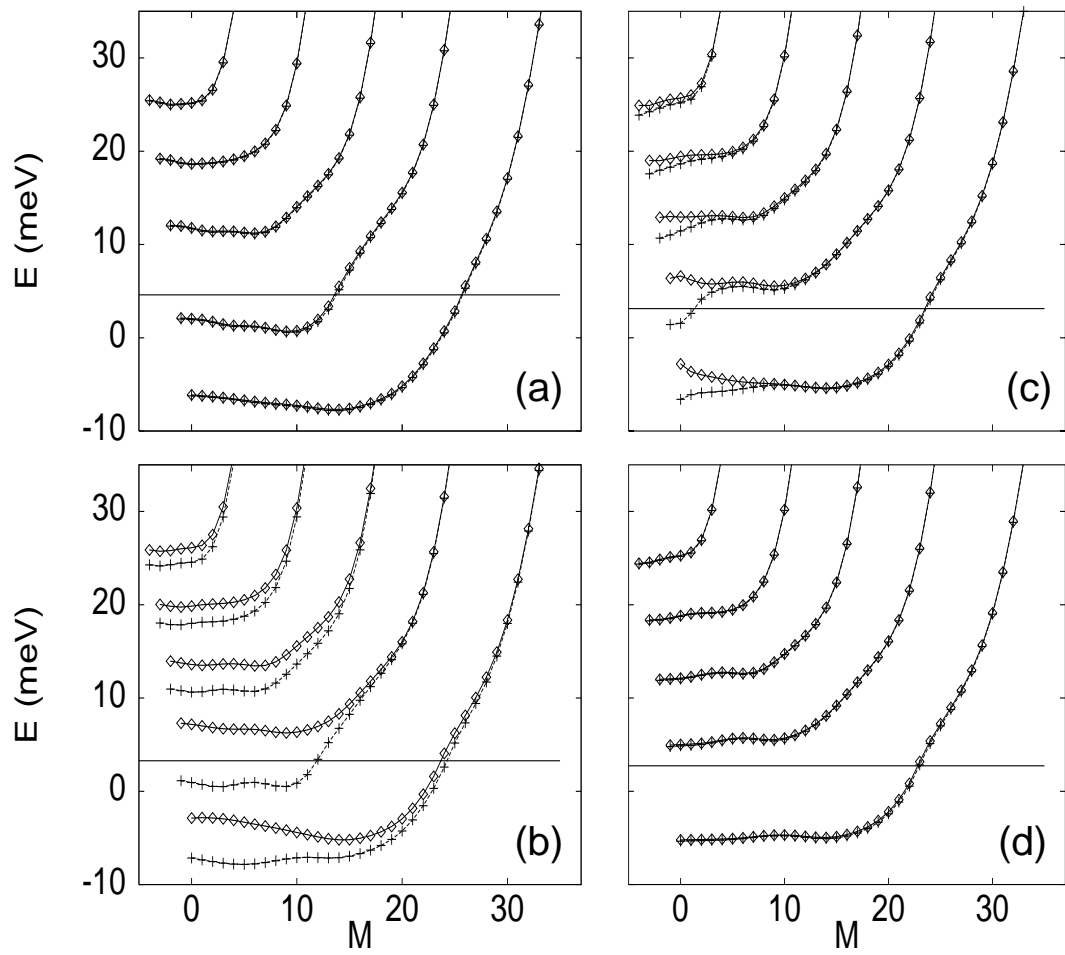
FIG. 3. The ground state electron density $n_s(r)$ for $s = -1/2$ (solid) and $s = +1/2$ (dashed) in the case of $T = 4.0$ K. Other parameters are as in Fig. 1.

FIG. 4. HFA ground state energy spectra and chemical potential μ for 30 electrons in a parabolic confinement potential at $T = 0$ K for (a) $\hbar\omega_c = 3.0$ meV, (b) $\hbar\omega_c = 5.0$ meV, and (c) $\hbar\omega_c = 7.0$ meV. Only one LB is considered. Confinement frequency $\hbar\omega_0 = 5.0$ meV. Crosses represent the $s = +\frac{1}{2}$ electrons and diamonds represent $s = -\frac{1}{2}$. Other parameters are as in Fig. 1.

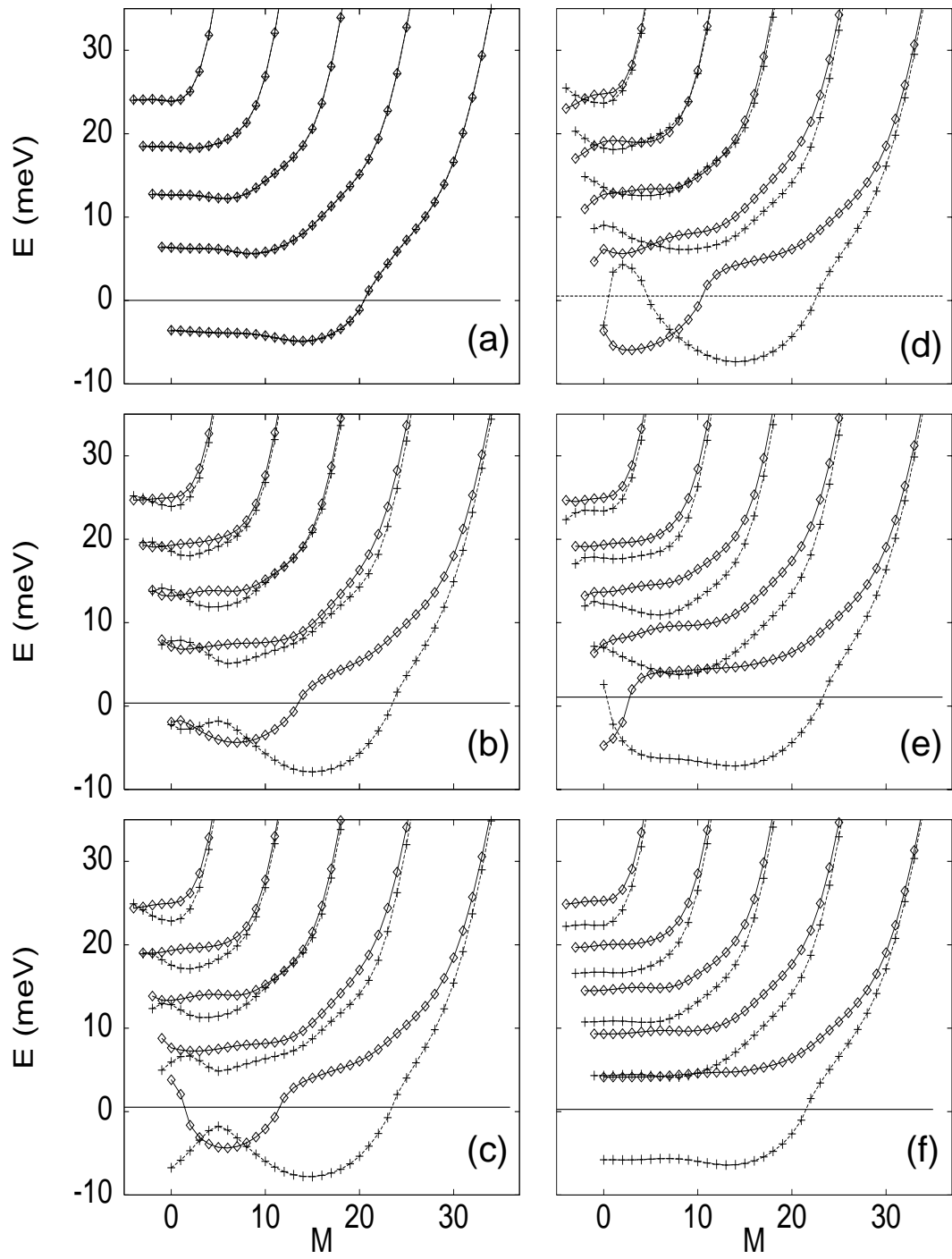
FIG. 5. HFA ground state energy spectra and chemical potential μ for 30 electrons in a parabolic confinement potential at $T = 1.0$ K. 1 LB is used for the calculation of the top sub-figure, 2 for the center one, and 3 for the bottom one. $\hbar\omega_c = 8.0$ meV, and the confinement frequency $\hbar\omega_0 = 4.0$ meV. Crosses represent the $s = +\frac{1}{2}$ electrons and diamonds represent $s = -\frac{1}{2}$. Other parameters are as in Fig. 1.

FIG. 6. The FIR-absorption $P(E)$ vs. E/E_c ($E_c = \hbar\omega_c$) and the number of electrons N_s for $N_p = \pm 1$ for HA (left), HFA (center), and for $N_p = -1$ in the HFA (right). $T = 4.0$ K and other parameters are as in Fig. 1.

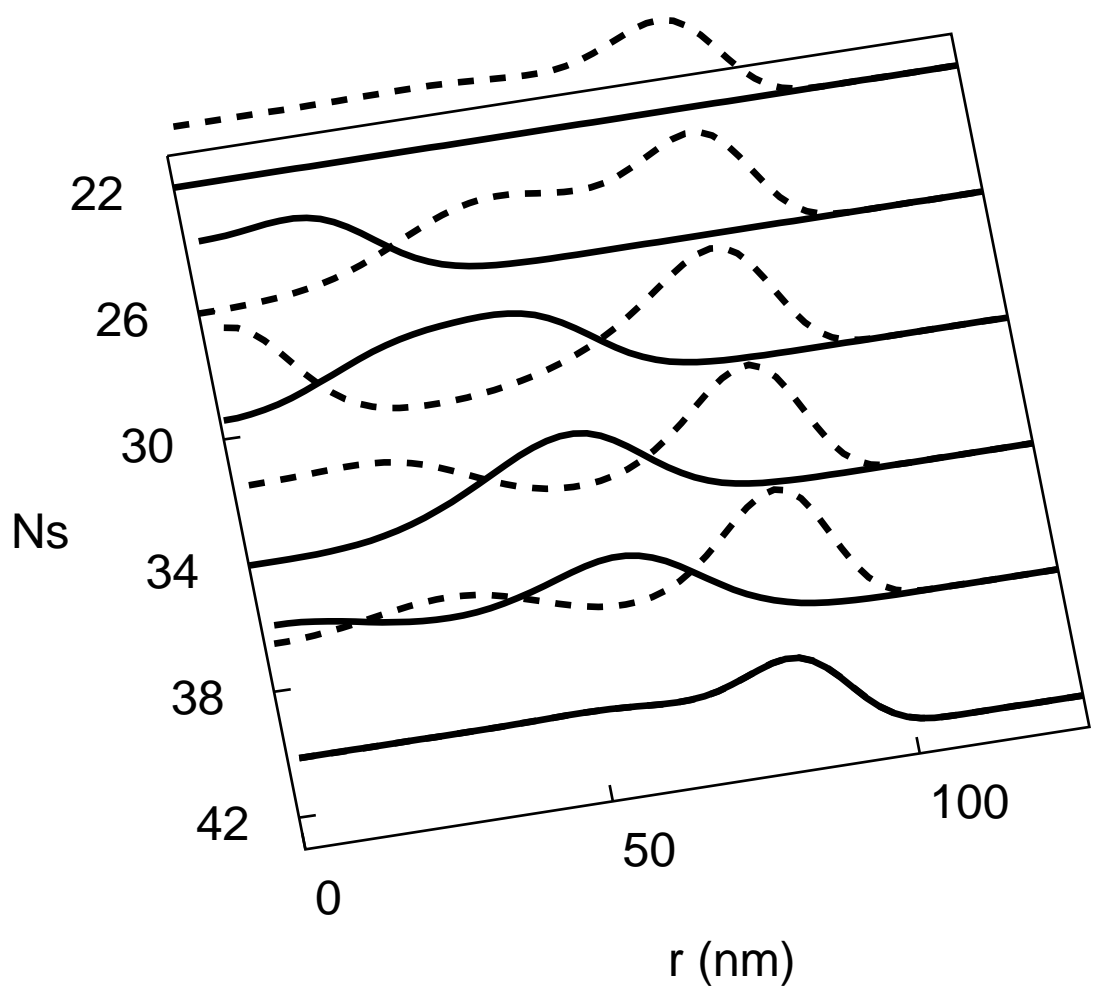
FIG. 7. Energy spectra and chemical potential μ (horizontal line) of several stable excited states for $N_s = 34$. Same parameters as in Fig. 2.



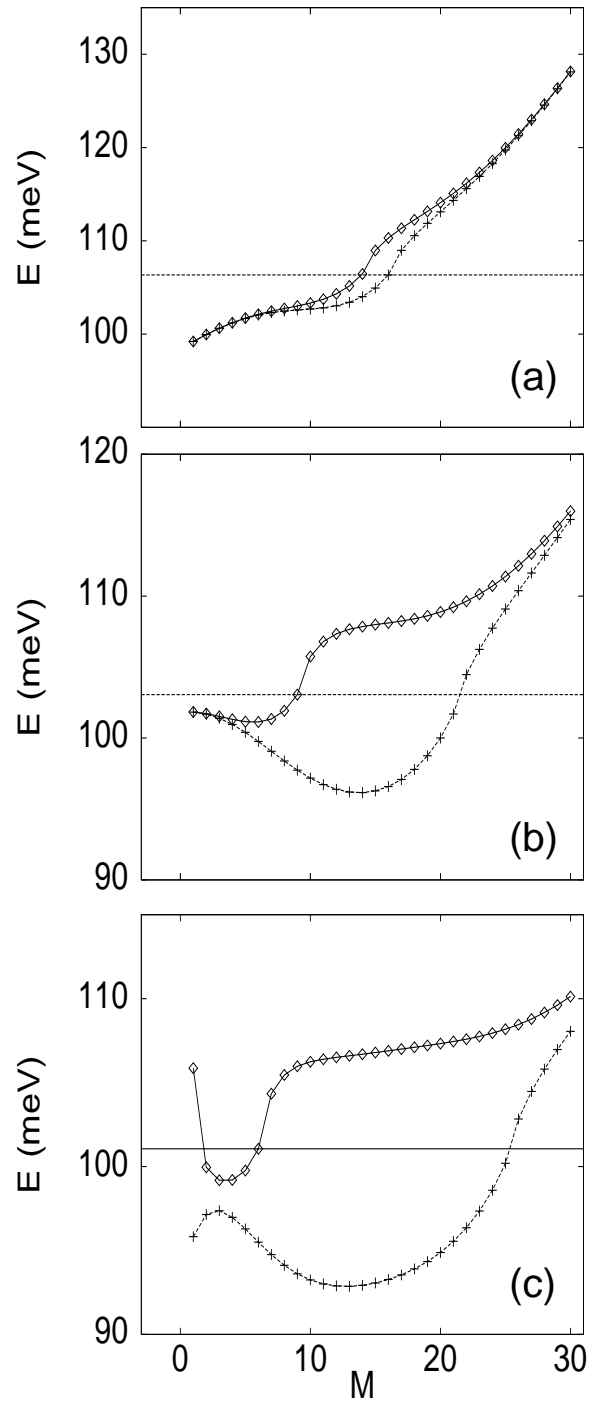
Gudmundsson, Fig. 1



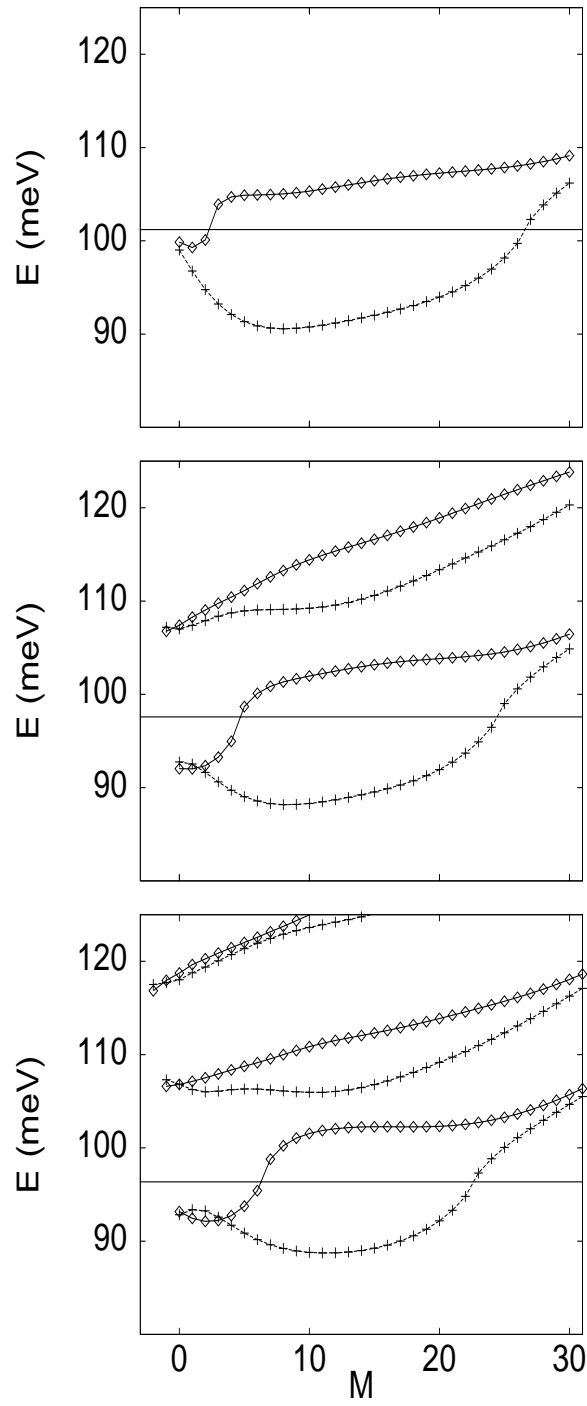
Gudmundsson, Fig. 2



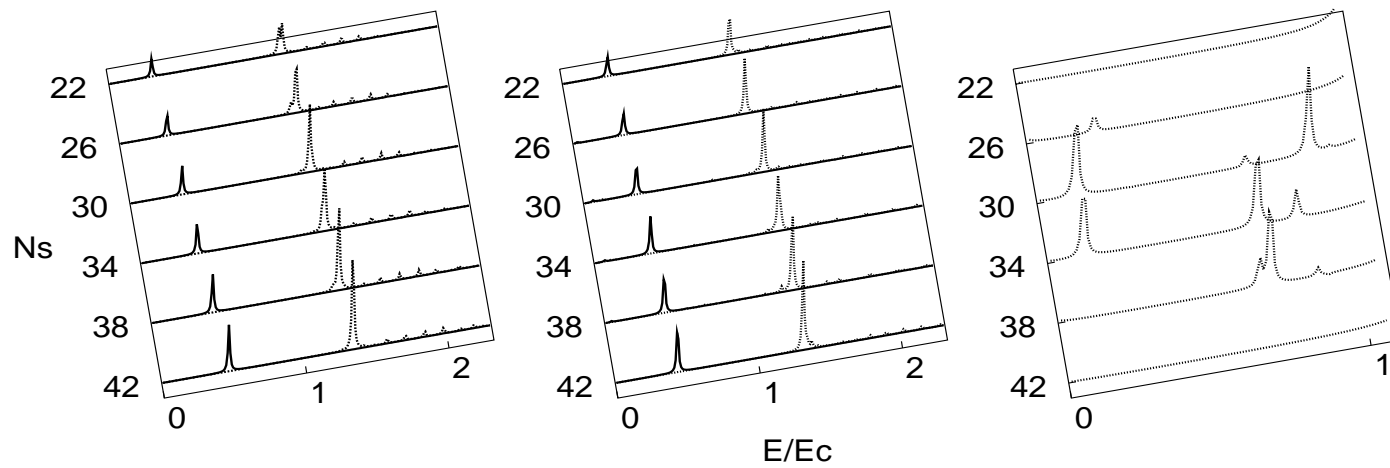
Gudmundsson, Fig. 3



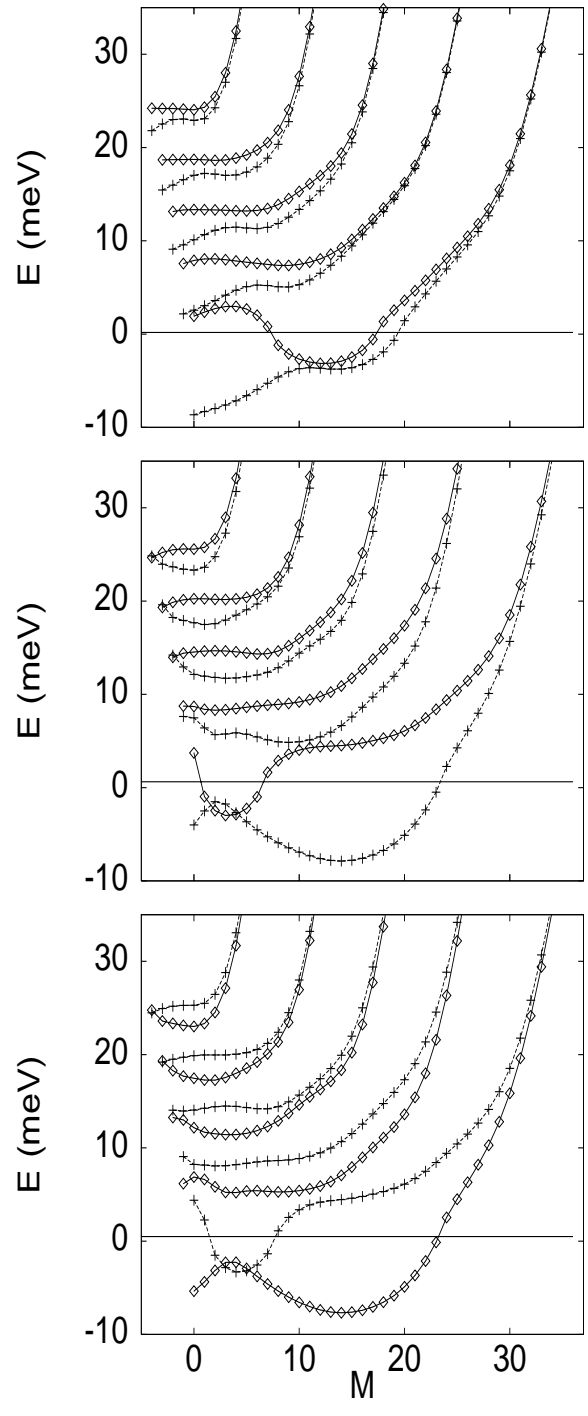
Gudmundsson, Fig. 4



Gudmundsson, Fig. 5



Gudmundsson, Fig. 6



Gudmundsson, Fig. 7